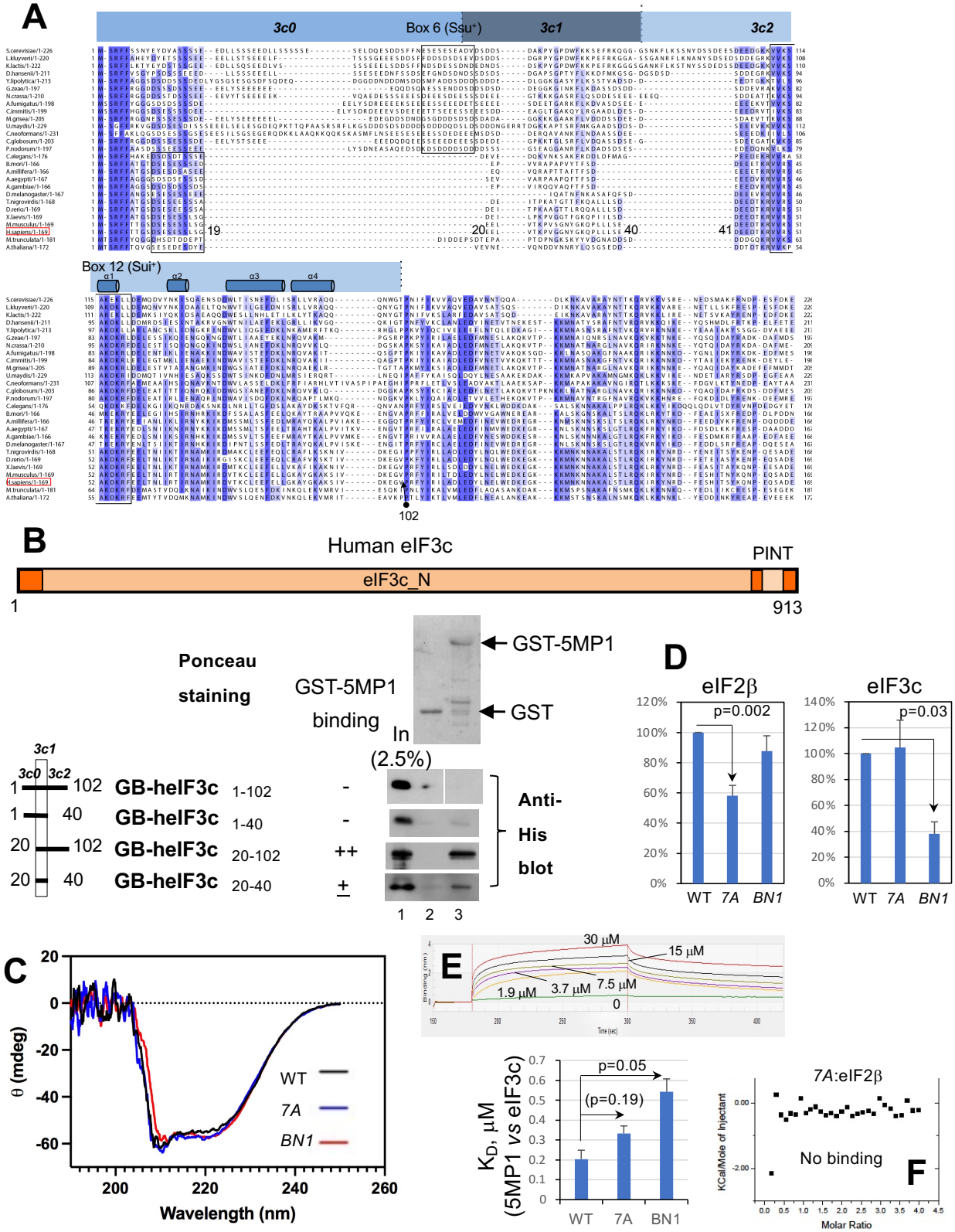
A
3c0
Box 6 (Ssu*)
3c1
3c2
Box 12 (Sui*)
α1
α2
α3
α4
102
B
Human eIF3c
PINT
eIF3c_N
1
913
Ponceau staining
GST-5MP1 binding
GST-5MP1
GST
In (2.5%)
Anti-His blot
1 2 3
3c1
3c0 3c2
GB-heIF3c 1-102
GB-heIF3c 1-40
GB-heIF3c 20-102
GB-heIF3c 20-40
D
eIF2β
eIF3c
p=0.002
p=0.03
WT 7A BN1
C
θ (mdeg)
Wavelength (nm)
WT
7A
BN1
E
30 μM
15 μM
7.5 μM
3.7 μM
1.9 μM
0
Time (sec)
KD, μM (5MP1 vs eIF3c)
p=0.05
(p=0.19)
WT 7A BN1
7A:eIF2β
No binding
F
Molar Ratio
KCal/Mole of Injectant

**Figure S1. 5MP1-binding regions in human eIF3c and supplementary analyses of *in vitro* 5MP1 interaction assays.** *Figure S1, related to Fig. 1.*

**(A)** The entire 102 aa eIF3c fragment N-terminal retains homologous structures previously subdivided into three regions, 3c0, 3c1 and 3c2, with yeast eIF3c/Nip1p. Alignment of eIF3c-NTD sequences from diverse eukaryotes, as reported in (Obayashi et al., 2017). *Homo sapiens* sequences are highlighted by red boxes. Numbers in *H. sapiens* sequence indicate the location of end points for deletion constructs used in this study. Cylinder symbols above the alignment indicate the location of $\alpha$-helices found in the region 3c2 (Obayashi et al., 2017). Boxes indicate the location of Box6 and Box12, previously identified in yeast as the $Ssu^-$ and $Sui^-$ mutation sites. Modified from Figure S1 in (Obayashi et al., 2017). **(B)** GST pulldown assays define the minimal 5MP1-binding region of human eIF3c. Schematic on top represents primary human eIF3c structure with the region of Pfam domains highlighted in lighter colored boxes. The lines beneath the schematic depict the location of four truncated heIF3c proteins fused to GB1, employed in this study (designated on the left). Table to the right of the schematic summarizes relative amount of these proteins bound to GST-h5MP1 (Singh et al., 2011), shown to the right. The GB-heIF3c proteins were expressed in *E coli* and their fractions bound to GST-5MP1 were detected by anti-His antibodies. **(C)** CD spectra of full-length recombinant h5MP1 proteins. **(D)** Graphs summarize the quantification of the amount of GB-heIF2$\beta_{53\text{-}136}$ and GB-heIF3$c_{20\text{-}102}$ bound to GST-5MP1 (WT) and its *7A* and *BN1* mutants (a representative result is shown in Fig. 1D). The amount bound to each GST fusion protein was shown by percentage compared to WT, with arrows indicating significant differences (n=3). (E) BLI experiments. GST-h5MP1 (WT), -*7A* or -BN1 attached to anti-GST biosensor chip was soaked into GB-heIF3$c_{20\text{-}102}$ at various concentrations. Top, a typical sensorgram showing GST-h5MP1 (WT) binding to GB-heIF3$c_{20\text{-}102}$ at indicated concentrations. Bottom, the summary of $K_D$ determined between the indicated GST-h5MP1 derivative and GB-heIF3$c_{20\text{-}102}$ (n=4). (F) An ITC experiment. Graph shows the integrated heats plotted against the molar ratio of titration of heIF2$\beta_{53\text{-}136}$ (200 $\mu$M) with h5MP1-*7A* at 20 $\mu$M.

*Note on Fig. 1A-B*: GST-5MP1 bound GB1-heIF3c$_{20-102}$ with high affinity, while having little to no binding affinity for the other eIF3c fragments (Fig. 1D-E and S1B). Thus, GB1-heIF3c$_{20-102}$ bearing 3c1 and 3c2 is determined to be a minimal human eIF3c segment capable of binding 5MP1. Curiously, GB1-heIF3c$_{1-102}$ carrying all three conserved segments did not bind GST-h5MP1 (top anti-His blot). This is in agreement with our previous data indicating that GST-heIF3c (full-length) did not bind h5MP1 (R. Watanabe and K. A., personal observation). Rather, this result suggests that the very N-terminus of heIF3c prevents its binding to h5MP1. Upon 5MP1 recruitment to the PIC, this inhibition would have to be resolved involving other parts of eIF3 or MFC.

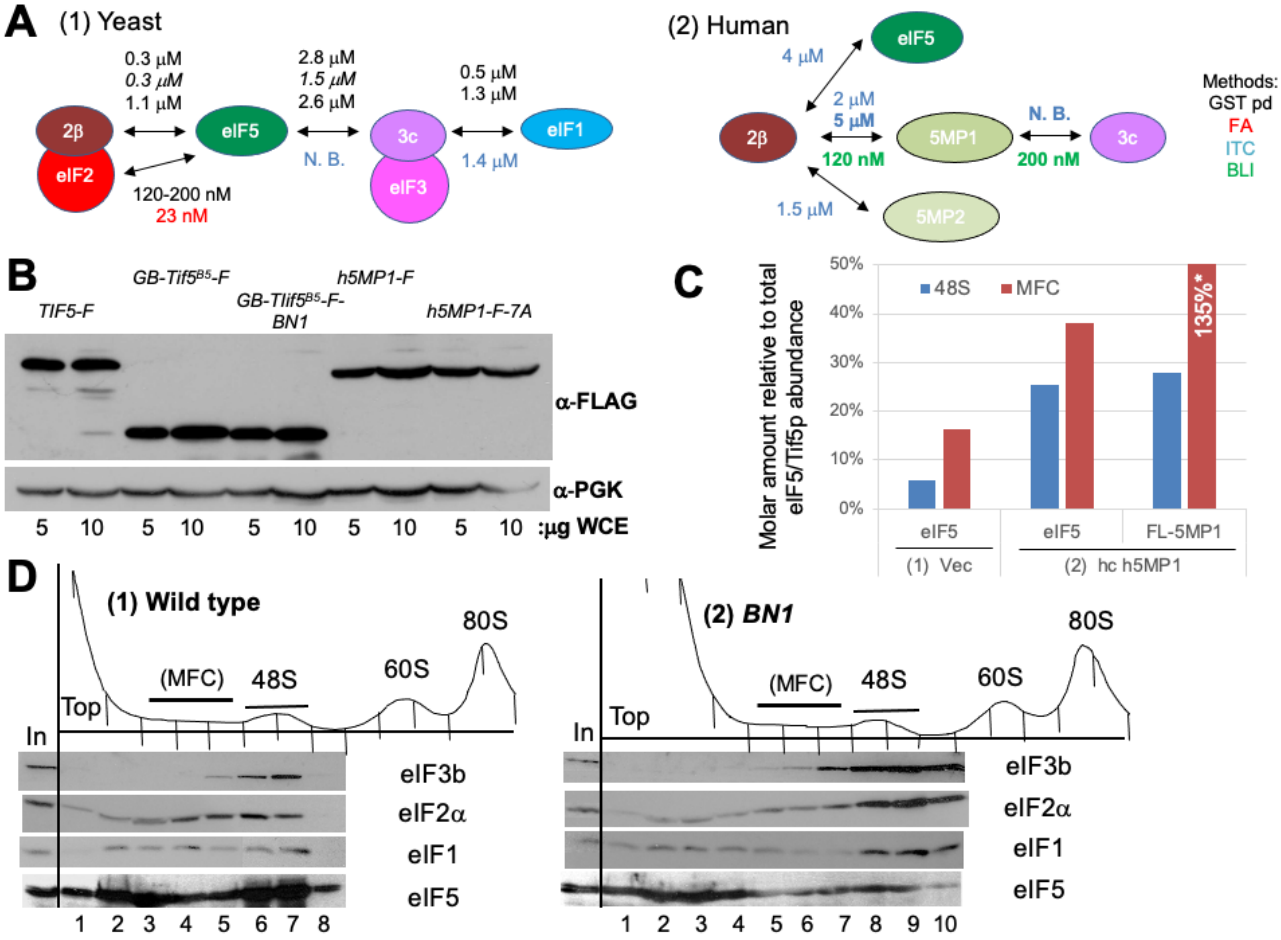


**Figure S2. Supplemental analyses of protein protein interactions studies *in vitro* and in yeast expressing h5MP1 and Tif5p/eIF5 derivatives.** *Figure S2, related to Fig. 1F and 2.*

**(A)** Summary of $K_D$ values obtained for interactions in MFC components in yeast and 5MP/eIF5 interaction with eIF2β or eIF3c in humans. Numbers in molar refer to $K_D$ in the experiments in color-code listed to the right (GST pd, Glutathine-S-transferase pull-down; FA, fluorescence anisotropy; ITC, isothermal titration calorimetry; BLI, bio-layer interferometry). GST pd was performed quantitatively with extra caution (Pollard, 2010; Singh and Asano, 2007). In panel 1, yeast proteins used are eIF2β/Sui3p$_{1-140}$, eIF5/Tif5p$_{241-405}$, eIF3c/Nip1p$_{1-156}$, and eIF1 in ovals color-coded as in Fig. 2, 4 and 7, except that full length eIF5 in combination with holo eIF2 (with α, β and γ subunits) and eIF3c$_{1-163}$ were used in FA (Algire et al., 2005)/GST pd (Singh et al., 2007) (tilted arrow) and ITC (Obayashi et al., 2017), respectively. On top, different $K_D$ values were obtained in GST pd (Singh et al., 2004) when GST is fused to the protein to the right (top value) or to the left (bottom value). Italicized value was obtained

with GB1-fusion to eIF5/Tif5p$_{241-405}$. In panel 2, human proteins were used; full-length eIF5 (Luna et al., 2012), 5MP1 (Hiraishi et al., 2014), and 5MP2 (Kozel et al., 2016) interacting with (GB-)heIF2$\beta_{53-136}$ or GB-heIF3c$_{20-102}$. Values from this study are boldfaced. N. B., no binding observed. **(B)** Transformants of KAY1027 (*sui1-G107R*, Sui$^-$) carrying hc plasmids with indicated TIF5/5MP1 alleles were grown in SC medium lacking leucine and subjected for preparation of whole cell extracts which are then used for immunoblotting with antibodies indicated to the right. Plasmids used are p313, p1206, p1263, p1587 and p1621 (Key Resource Table) from left. **(C)** Quantification of eIF5 and h5MP1-F abundances in 48S PIC and free MFC fractions in Fig. 2A, panels 1 and 2. Relative molar abundances of eIF5 and h5MP1-F were determined by ImageJ with the band density of lane 1 (1% input amount) as reference. h5MP1-F abundance was determined based on 80% OE level of h5MP1-F compared to Tif5-F in panel A and the fact that Tif5-F OE from the same plasmid produces 20-fold more Tif5p compared to the endogenous Tif5p (Asano et al., 1999). *, the amount of the FLAG-tagged h5MP1 likely includes its proportion outside of MFC, such as those found in h5MP1-eIF2 or h5MP1-eIF2-eIF2B complexes. **(D)** Effect of *tif5-BN1* on 40S subunit binding. KAY113 (Wild type) or KAY359 (*BN1*) (Yamamoto et al., 2005) were grown in YPD medium at 30$^o$ C and subjected to polysome analysis on a 15-40% sucrose gradient as described previously (Singh et al., 2004). $A_{254}$ profile is shown on top of each panel. One-third of top to middle fractions encompassing free eIFs and 40S ribosomes were analyzed by SDS-PAGE and immunoblotting with anti-eIF3b (Cigan et al., 1991), anti-eIF5 (Huang et al., 1997), anti-eIF2$\alpha$ (Dever et al., 1995) and anti-eIF1 (von der Haar and McCarthy, 2002) antibodies, indicated to the right of each panel, together with 1% of in-put amount used for loading on the sucrose gradient (lanes labeled “I”). Shown is a typical result from three independent experiments. (MFC), free MFC does not accumulate in yeasts grown in YPD when compared to those grown in SC (see Fig. 2A for example) (Singh et al., 2007).

*Notes on Fig. 2A*: As shown in Fig. 1F, the $K_D$ values obtained for the h5MP1(WT): heIF2$\beta_{53-136}$ interaction is quite different between ITC and BLI. This, although not unique, requires further attention. GST fusion proteins form a dimer, which is known to overestimate affinity through avidity effects (one GST dimer binds to two immobilized molecules) in, for example, surface plasmon resonance (Ladbury

et al., 1995). Although we avoided avidity effects in our BLI approach through immobilizing GST-h5MP1 fusion into the sensor, GST-h5MP1 dimer formation could still increase the overall affinity. Nevertheless, to examine this and other discrepancies in $K_D$ measurements, including ITC, in particular, we compared the $K_D$ values obtained by various experiments for mutual interactions between yeast MFC components and human 5MP interactions with eIF2β or eIF3c (Fig. S2A, panels 1 and 2). $K_D$ obtained previously for h5MP1: (GB-)heIF2$\beta_{53-136}$ complex was 2 μM (Hiraishi et al., 2014), 2.5-fold lower than in this work (panel 2). Most probably, the difference could be due to using untagged heIF2$\beta_{53-136}$ in this work.

It is noteworthy to find that the $K_D$ of 1.4 μM obtained for yeast eIF3c-NTD:eIF1 complex from ITC (Obayashi et al., 2017) matches with a value obtained with the conventional GST pull-down assays (panel 1) (Singh et al., 2004). However, ITC failed to detect interaction between eIF3c-NTD and full-length eIF5 (Eiji Obayashi and KA, unpublished observation), even though a discreate 4.3S complex was observed between the same proteins in analytical ultracentrifuge (Obayashi et al., 2017). Likewise, ITC failed to detect interaction between GB-heIF3c$_{20-102}$ and h5MP1 (CE, RJ and KA, unpublished observation) even though BLI showed a $K_D$ of 200 nM (Fig. S2A, panel 2, and Table 1). Provided that the pull-down assays are strongly biased towards dissociation (e. g., see comparison with fluorescence anisotropy data for eIF5:eIF2 complex in panel 1), it could be interpreted that the ITC tends to give a higher $K_D$ value, as far as interactions in MFC components or 5MP interactions with them are concerned. Among many possibilities, this could be due to compensation by heat exchange due to intramolecular interactions that happen in the same system. The NTDs of eIF3c and eIF2β are strongly charged and yet embedded with conserved hydrophobic residues. Therefore, these protein segments may tend to undergo intramolecular conformational changes upon binding to their partners.

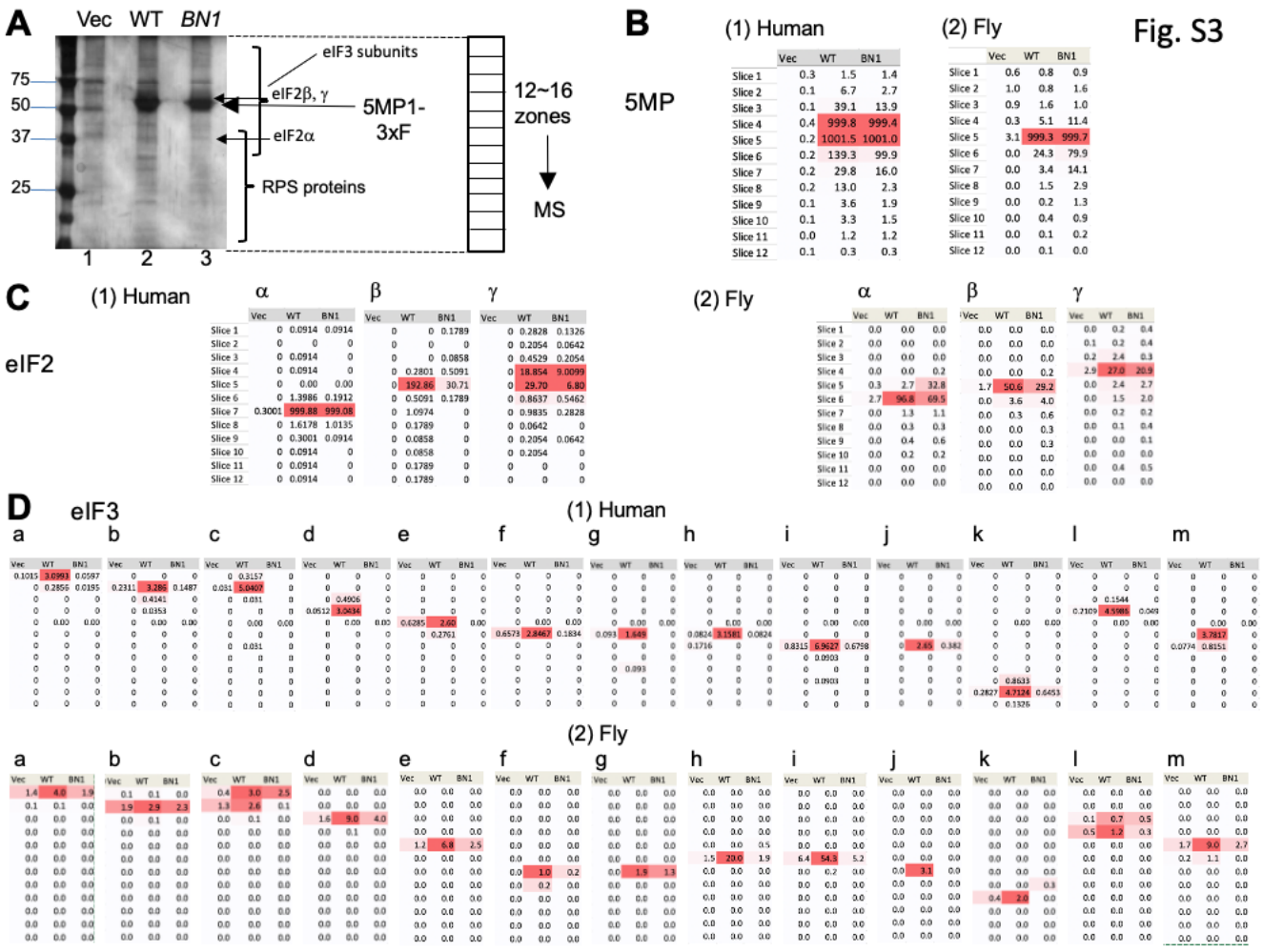


**Figure S3. MS analysis of FLAG-h5MP1 complexes.** *Figure S3, related to Fig. 4A-C.*

**(A)** Scheme for MS analysis of FLAG-h5MP1 complexes. Samples of triple-FLAG (3xF-) tagged h5MP1 WT and h5MP1-*BN1* complexes and its vector transfection control (Vec) were separated by SDS-PAGE and stained with silver (lanes 1-3). Shown to the right by arrows is the identity of stained proteins deduced from previous analysis of WT h5MP1 complex (Kozel et al., 2016). Each lane of the gel was divided into 12~16 zones, excised and subjected for MS analysis. **(B-D)** Summary of emPAI values for 5MP (B) and the subunits of eIF2 (C) and eIF3 (D) from a typical set of anti-FLAG affinity purification experiments in human (panels 1) and fly (panels 2). emPAI values are listed for each gel slice. The gradient of red color is set to indicate the intensity of protein detection.

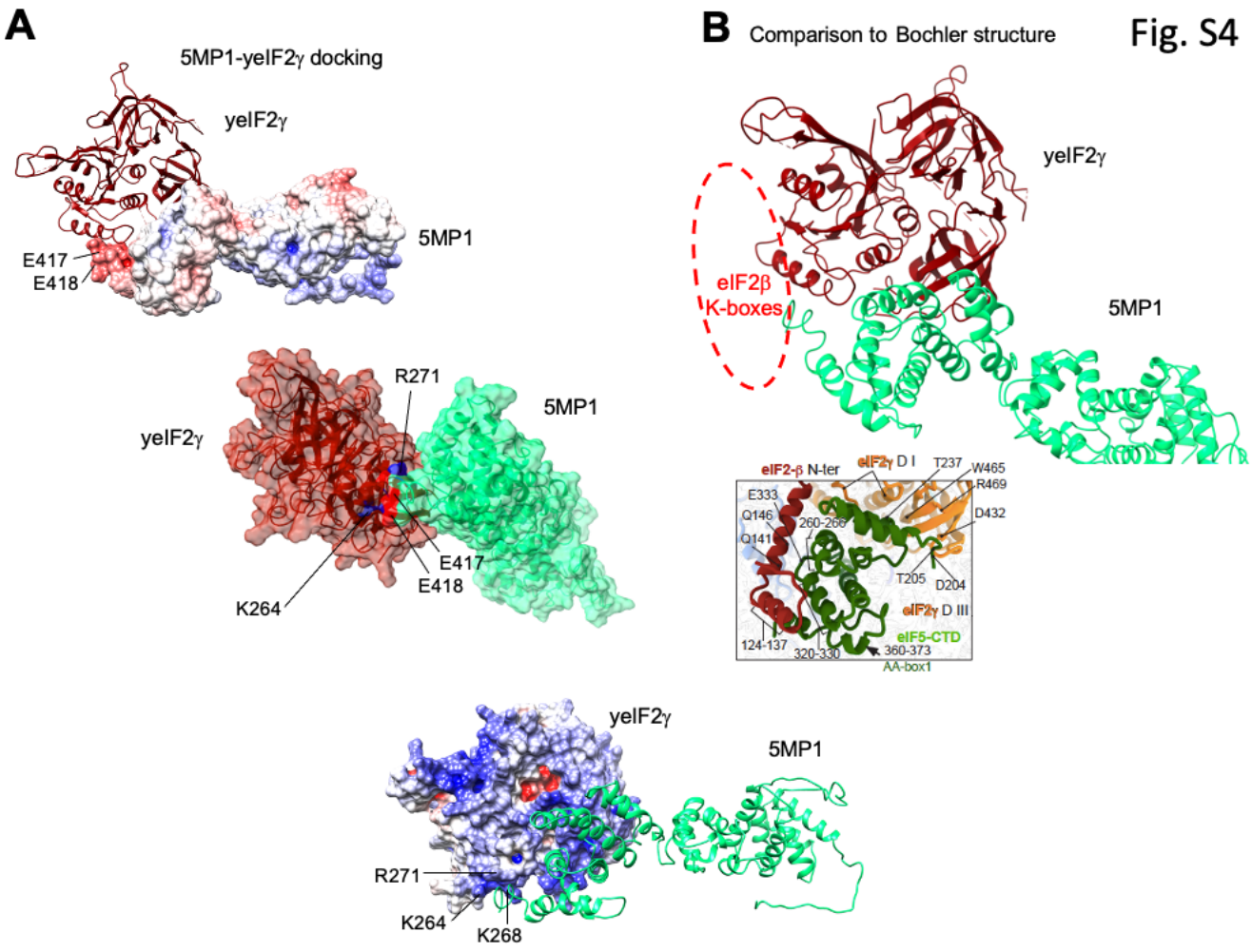


**Figure S4. Homology model of 5MP1 and its complex with eIF2γ.** *Figure S4, related to Fig. 4D.*

Structure of h5MP1 (green): yeIF2γ (red) complex were generated by docking studies (see Supplementary Methods). **(A)** h5MP1 and yeIF2γ are shown in ribbon diagrams, except for each shown in surface presentations with negative (red) and positive (blue) charges in the left and right panels, respectively. In the middle, the structure is overlaid with semi-transparent surface presentations. h5MP1 residues Glu-417, Glu-418 and yeIF2γ residues Lys-264, Lys-268, and Arg-271, which are predicted to interact together, are highlighted. **(B)** The ribbon-presentation of the complex (top) is viewed from a similar angle compared to the presentation of eIF5:eIF2γ complex in the Trypanosoma cryoEM PIC structure (Bochler et al., 2020) shown below in box. Red dotted circle indicates the location of eIF2β-NTD K-boxes deduced from the Trypanosoma structure.

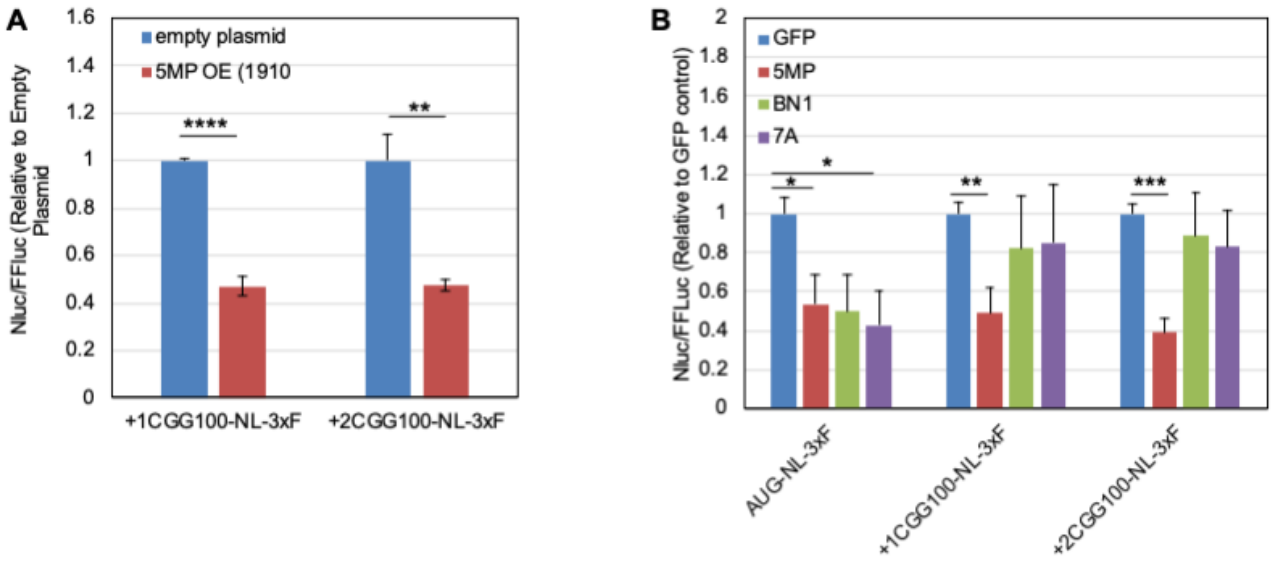


**Figure S5. Additional analysis of 5MP1 regulation of RAN translation.** *Figure S5, related to Fig. 5.* (A) Expression of nLuc-3xF tagged RAN translation reporters was examined after cotransfection in HEK293T with a firefly luciferase control plasmid and an empty vector or p1910 expressing 5MP1 from the CMV promoter (Key Resource Table), distinct from 5MP1 expression vector used in Fig. 5. Bars represent mean +/-stdev, N=3. **p<0.01, ****p<0.0001. (B) Similarly, expression of nLuc-3xF tagged RAN translation reporters was examined in HEK293T after cotransfection with a firefly luciferase control plasmid and GFP-2A-mCherry (GFP), 5MP1-2A-mCherry (5MP), 5MP1-*7A*-2A-mCherry (7A), or 5MP1-*BN1*-2A-mCherry (BN1) fusion plasmid (Key Resource Table). Expression of the fusion protein follows the spontaneous cleavage between mCherry and its fusion partner. Bars represent mean +/-S.E.M, N=6. *p<0.05, **p<0.01, ***p<0.001.

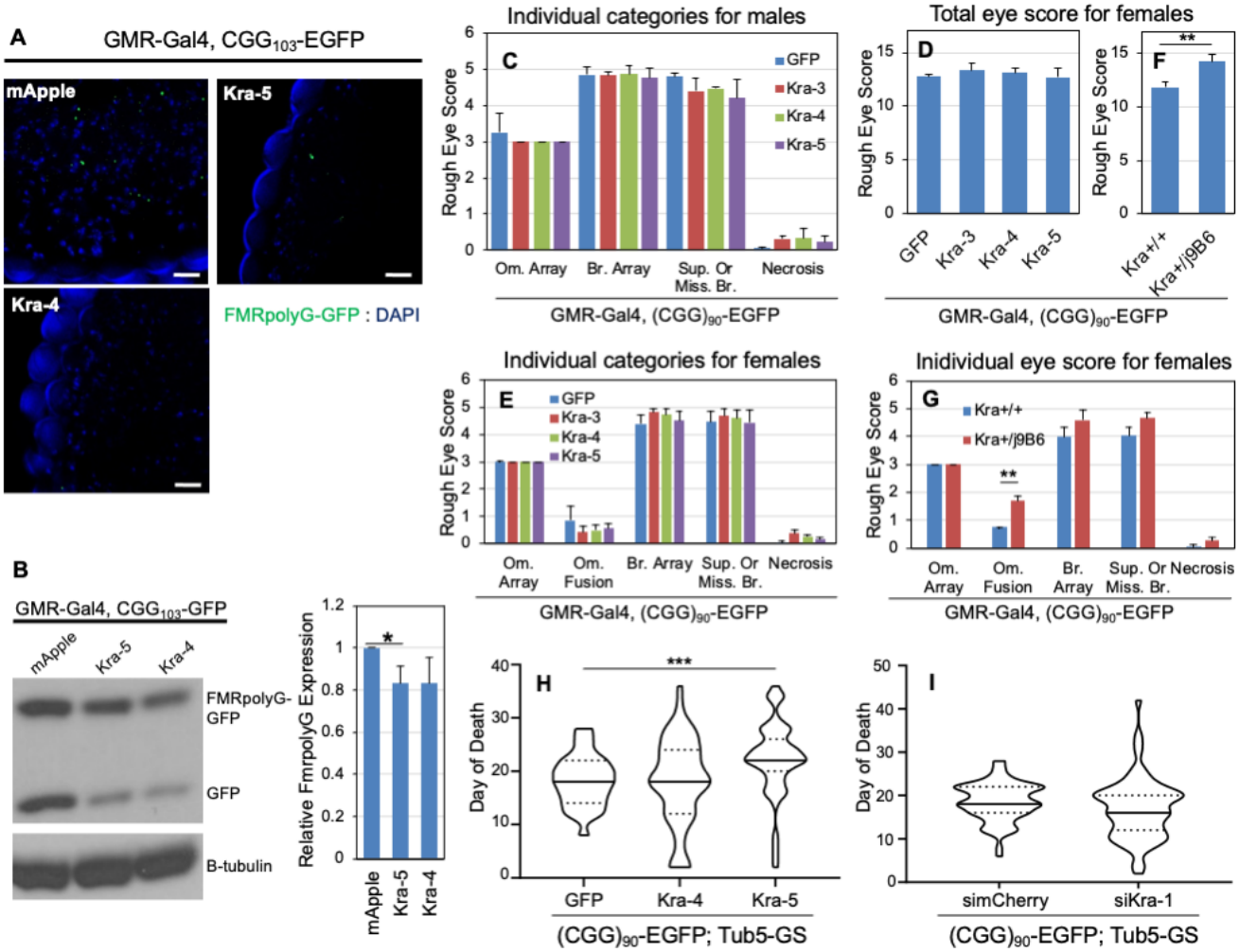


**Figure S6. Supplemental analysis of *Drosophila* 5MP.** *Figure S6, related to Fig. 6.*

**(A)** Representative IHC images of FMRpolyG aggregates in the indicated fly lines. Image thickness: 5um, Scale bar: 10um. N=>7/genotype **(B)** *Right* Western blot of lysates from heads of 1-3 day old *Drosophila* of the indicated genotypes. *Left quantification of western blot.* N=3, *p<0.05, unpaired t-test. **(C)** Quantification of male individual rough eye category phenotypes of GMR-GAL4, $(CGG)_{90}$-EGFP crossed to Kra OE lines. Bars represent mean +/- stdev for 3 individual experiments (N≥25/genotype/experiment with the exception of 1 experiment for Kra-5 (N=10)). Two-tailed Welch's t-test with Bonferonni correction. **(D-E)** Quantification of female total eye phenotype (D), and individual category phenotypes (E) of GMR-GAL4, $(CGG)_{90}$-EGFP crossed to Kra OE. (N≥23/genotype/experiment with the exception of 1 experiment for Kra-4 (N=12). **(F-G)** Quantification of female total eye phenotype (F), and individual category phenotypes (G) of GMR-GAL4, $(CGG)_{90}$-

EGFP crossed to WT or Kra disruption lines. (N≥15/genotype/experiment). (C, E, F & G) Two-tailed Welch's t-test with Bonferonni correction. (D) One-way ANOVA=*** with Dunnett's multiple-comparison test. **(H-I)** Quantification of survival of female flies expressing $(CGG)_{90}$-EGFP under GMR-GAL4 with H) Kra OE or I) siKra. Solid lines represent median day of death, dotted lines represent 25% and 75% quartiles, for N≥51/genotype (from 2-3 experiments/genotype). Two-tailed Welch's T-test with Bonferonni correction. **p<0.01, ***p<0.001. GFP and simCherry serve as controls.

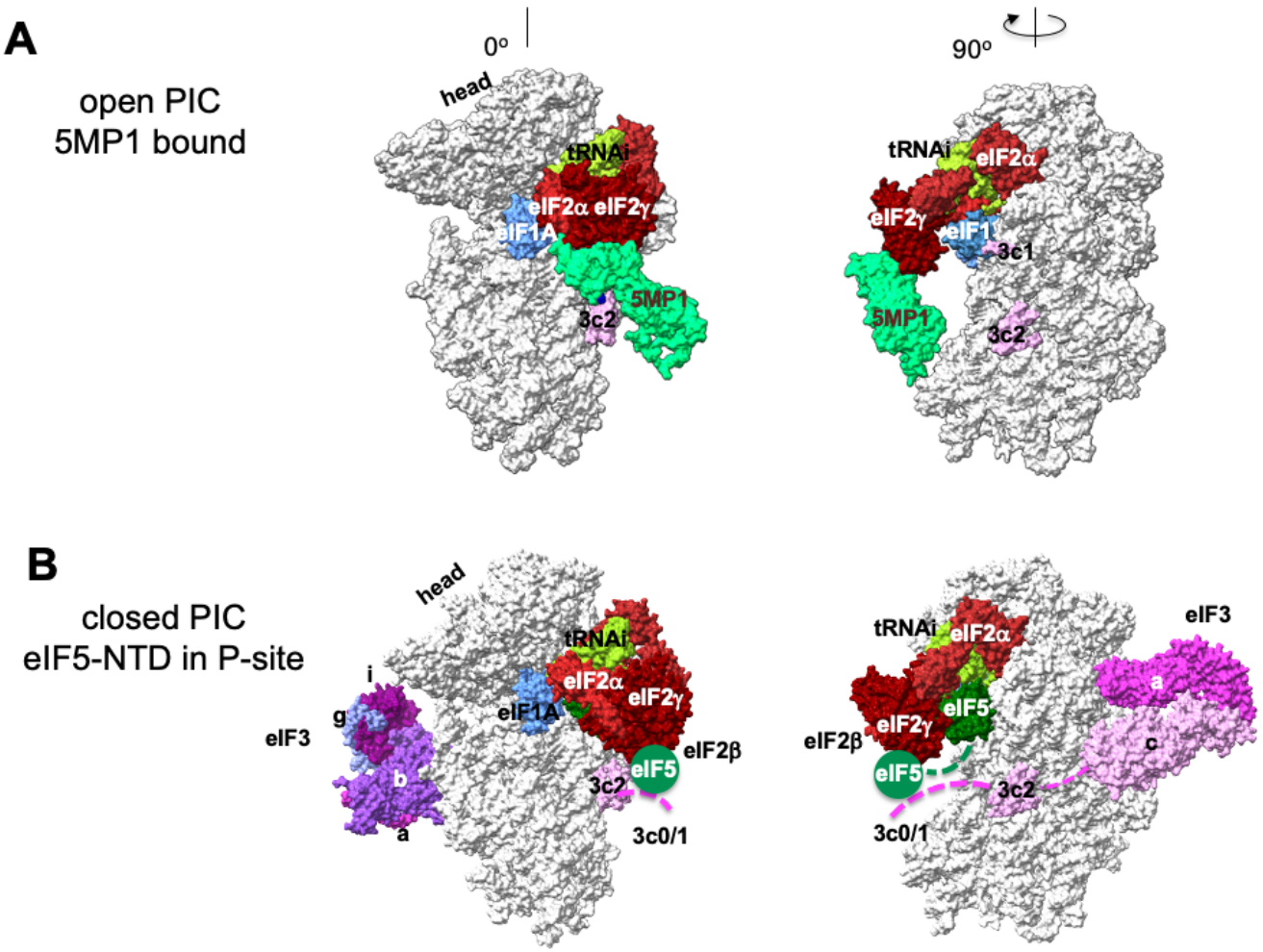


**Figure S7. Comparison of 5MP-loaded PIC (A) and the closed PIC with eIF5-NTD in the P-site (B).**

*Figure S7, related to Fig. 7.*

In (A), h5MP1 was docked onto eIF2γ of the open PIC structure (3JAQ). See Supplementary Methods for details. The structure shown in (B) is based on 6FYX painted with the same color codes for initiation factors as the open structure.